

Soft x-ray laser holography with wavelength resolution

P. W. Wachulak, M. C. Marconi,* R. A. Bartels, C. S. Menoni, and J. J. Rocca

NSF Engineering Research Center for Extreme Ultraviolet Science and Technology and Department of Electrical and Computer Engineering, Colorado State University, Fort Collins, Colorado 80523, USA

*Corresponding author: marconi@engr.colostate.edu

Received August 18, 2008; accepted August 26, 2008;
posted September 3, 2008 (Doc. ID 100162); published October 13, 2008

We report the tabletop acquisition of soft x-ray holographic images of nanostructures with a spatial resolution of 46 ± 2 nm, nearly equal to the wavelength of the illumination. Holograms of carbon nanotubes were recorded using a compact, tabletop capillary-discharge soft x-ray laser emitting at 46.9 nm in a high-numerical-aperture Gabor configuration. © 2008 Optical Society of America
OCIS codes: 090.1995, 340.7480, 140.7240, 180.7460.

1. INTRODUCTION

The ability to acquire sub-50-nm resolution holograms of nanoscale objects with a compact light source in a tabletop setup could represent a significant contribution in nanoscience and nanotechnology. Shortly after the introduction of in-line holography by Gabor [1], the feasibility of holographic imaging in the x-ray region with a resolution superior to that obtained by optical microscopy was discussed by Baez [2]. The first demonstration of holographic imaging at soft x-ray wavelengths achieved a spatial resolution of $5\ \mu\text{m}$ making use of an early laboratory-size soft x-ray laser pumped by a fusion-class laser [3]. Subsequently, synchrotron radiation has been used in holographic imaging of biological samples and nanostructures [4–7]. Recently, significantly more-compact, tabletop soft x-ray lasers and high harmonic sources have been used to realize demonstrations of holographic imaging [8–10]. However, the lateral spatial resolution achieved has remained far from the wavelength of the illumination.

Herein we report high-resolution, soft x-ray holographic images of nanostructures with a spatial resolution of 46 ± 2 nm, practically equal to the wavelength of the illumination. Holograms of carbon nanotubes (CNTs) were recorded using a compact, tabletop capillary-discharge soft x-ray laser emitting at 46.9 nm in a high-numerical-aperture Gabor configuration. These are, to our knowledge, the highest spatial resolution holograms obtained with a tabletop setup, and also constitute the first demonstration of soft x-ray holography with wavelength resolution.

2. EXPERIMENT

The hologram's lateral resolution is ultimately determined by the wavelength of the illumination λ and the numerical aperture NA, which for a given detector is set by the object-recording medium distance. However, the

temporal and spatial coherence of the illuminating source, the resolution of the medium in which the hologram is recorded, and the digitization process used are also factors that influence the ultimate resolution. The experimental setup described in this paper was optimized to limit the degrading effect of these factors on the image resolution.

A sample composed of CNTs with diameters between 50 and 80 nm and a length between 10 and 20 μm , placed on a 100 nm thick silicon membrane, was imaged using a tabletop soft x-ray laser in a Gabor's in-line configuration shown in Fig. 1(a). The thin Si membrane has a transparency of approximately 60% at $\lambda=46.9$ nm [11]. The CNT sample was placed at approximately 2.6 μm away from a Si wafer spin-coated with a 120 nm thick layer of polymethyl methacrylate (PMMA) photoresist providing a NA practically equal to 1. However, the limited area of the atomic force microscope (AFM) scan that digitizes the hologram ($9.9\times 9.9\ \mu\text{m}^2$) reduces the effective value to $\text{NA}=0.88$. The CNTs were illuminated by a compact $\lambda=46.9$ nm capillary discharge Ne-like Ar soft x-ray laser [12,13]. To ensure its proper reconstruction, the hologram, recorded as a relief modulation in the photoresist surface, was exposed with a dose within the linear response regime of the photoresist. The developed photoresist surface was mapped with an AFM to generate digitized holograms that were reconstructed by numerically simulating the illumination with a soft x-ray readout wave. The amplitude and the phase distribution of the field in the image plane were obtained by calculating the field emerging from the hologram illuminated by a plane reference wave and numerically backpropagating the fields with a Fresnel propagator [14]. The reconstructed image was found by taking the two-dimensional inverse fast Fourier transform (2D-FFT) of the product of the spatial frequency of the Fresnel propagator and the 2D-FFT of the hologram.

Figure 2(a) shows a hologram digitized with the AFM. The corresponding numerical reconstruction processed

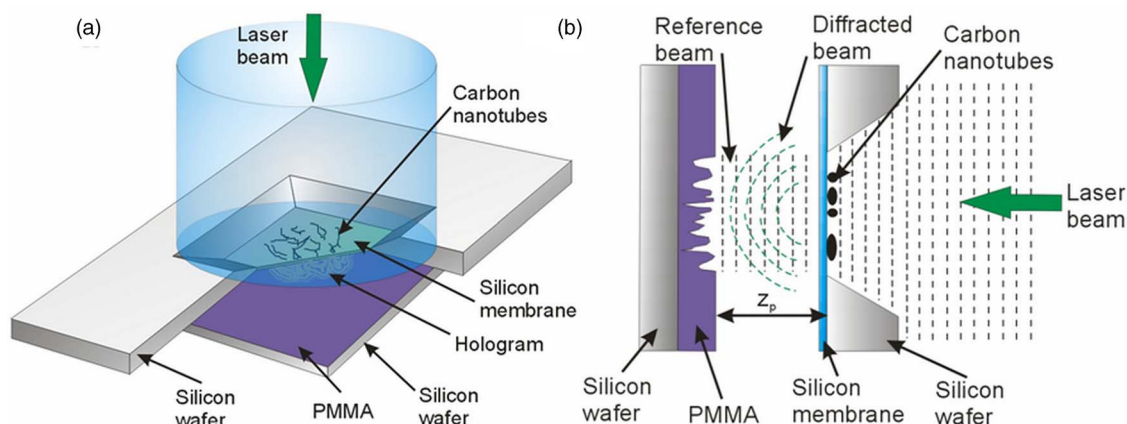


Fig. 1. (Color online) Experimental setup. (a) Gabor's hologram configuration. The soft x-ray laser beam illuminates the object composed of carbon nanotubes deposited in a Si membrane. The recording medium is a high-resolution photoresist. (b) Side view of the setup. After developing, the intensity modulation is converted into a height modulation in the photoresist surface.

with a Fresnel propagation code is shown in Fig. 2(b). The CNTs are clearly distinguishable as white lines in a black background. The spatial resolution in the reconstructed image was evaluated by use of the knife-edge method based on measuring the 10–90% rise of the intensity in line-cuts through the image. An example of such a line-cut as indicated in Fig. 3(a) is shown in Fig. 3(b). Figure 3(a) is a zoom-out of the region indicated in Fig. 2(b) with a white dotted square. This cut, realized in a region where we clearly reached a “plateau” in the maximum and minimum intensities to recreate the knife-edge resolution test, yielded a resolution of 46 nm. An average of similar cuts realized in different points of the image result in a resolution 45.8 ± 1.9 nm where the error is assigned by the standard deviation spread in the measurements. To obtain a global assessment of the image spatial resolution, a correlation analysis of the reconstructed holograms was performed [15]. This method is based on the correlation between the reconstructed holographic image and a set of templates with calibrated resolution generated from a master binary template. The set of master binary tem-

plates is derived from the original image by skeletonization of the image and convolution with circular templates of different diameters, which represent different CNT diameters. From these master binary templates, a subset of templates with calibrated resolution was obtained by applying a Gaussian filter of increasing width. Figure 4 shows an example of these templates and the 2D correlation map that indicates that the CNT diameter is 70.6 ± 5 nm and the spatial resolution 47.5 ± 5 nm, where the error is assigned to the variation on one step in the calculation of the surface shown in Fig. 4(d).

The obtained resolution exceeds by ~ 19 – 21 nm the best possible obtainable resolution of 27 nm set by $\lambda/2$ NA [4]. Several factors contribute to degrade the resolution. We verified that the coherence of the laser source does not constitute a limitation in this experiment. The temporal coherence of the soft x-ray laser is approximately $\Delta\lambda/\lambda \approx 10^{-4}$, and the spatial coherence radius is approximately 0.25 mm at the location of the recording, 0.75 m from the source [16]. With these parameters, the spatial resolution set by the laser coherence properties is

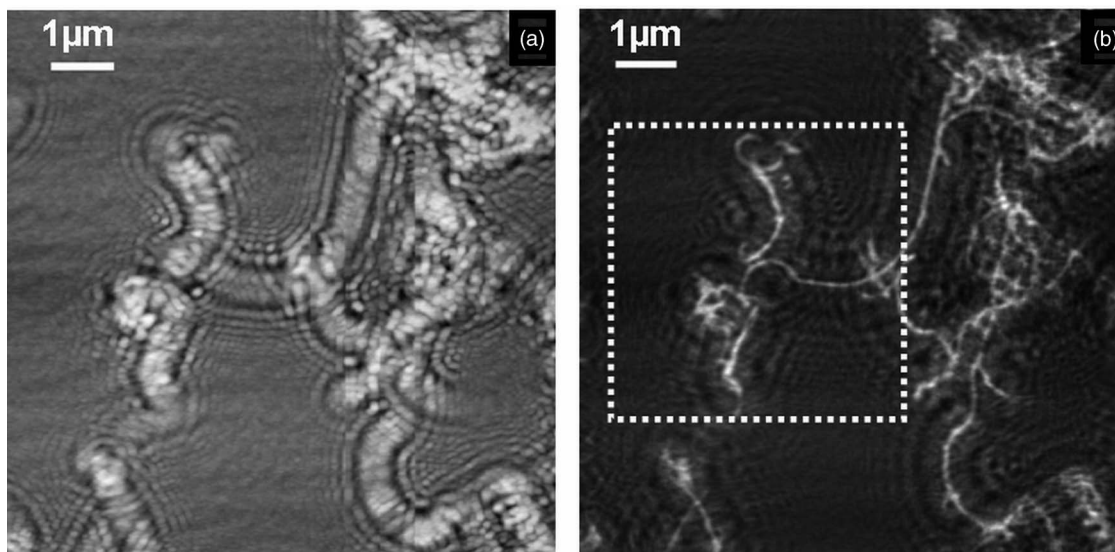


Fig. 2. (a) Hologram and (b) reconstructed images of 50–80 nm diameter carbon nanotubes. The holograms were obtained by scanning the photoresist surface with an AFM. The dotted square indicates the zoomed region in Fig. 3(a).

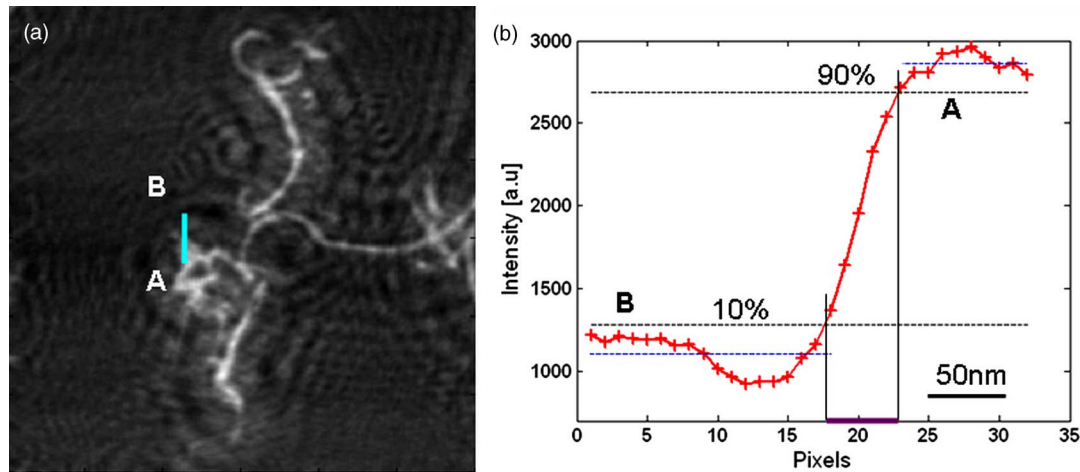


Fig. 3. (Color online) Knife-edge test applied to estimate the resolution of the image. The intensity lineout through the image from A to B is shown in (b) indicating a 10–90% intensity modulation over approximately 4.5 pixels. An average of multiple cuts obtained at different locations yielded a resolution of 45.8 ± 1.9 nm.

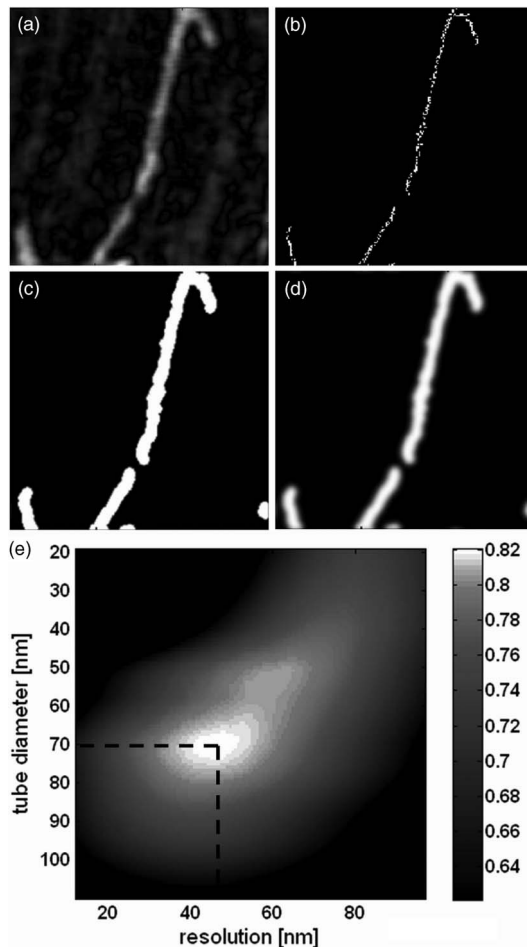


Fig. 4. Procedure to generate the templates with calibrated resolution. (a) Filtered image to remove the low-frequency background fluctuations. (b) Skeletonizing of the image. (c) Binary template obtained by convolution of skeleton template (b) with a circular template. (d) Template with degraded resolution obtained by convolution of the binary template (c) with a 2D Gaussian filter. (e) Correlation coefficients of the image with the different templates plotted as a function of the nanotube diameter and template resolution. The nanotube diameter and resolution of the image are determined to be 70.6 ± 5 nm and 47.5 ± 5 nm, respectively, by localizing a global maximum in the correlation plot.

approximately 29 nm [9]. Another limiting factor could arise from the digitization. The AFM maps the hologram into a 1024×1024 matrix over a surface of approximately $9.9 \times 9.9 \mu\text{m}^2$, giving a pixel size of 9.7 nm. This pixel size sets the maximum spatial frequency that can be recorded, thus establishing a limit for the spatial resolution of ~ 12 nm that does not play a practical role in our experiment. However, the resolution is affected by the photorealist resolution (estimated to be ~ 20 nm [17]) and by the resolution of the AFM that is defined by the 10 nm radius of curvature of the tip. The latter is not a fundamental limitation, as it can be overcome using a high-resolution AFM tip. Convoluting these factors, the best possible resolution in our experiment is estimated to be ~ 39 nm, which is slightly better than the observed resolution. An additional possible factor degrading the resolution is the roughness of the Si membrane. Variations in the membrane's thickness can introduce a random background noise that degrades the image resolution. Detailed modeling indicates that a surface roughness of ~ 20 nm, which is similar to the measured roughness of the wafer that contains the membrane, would degrade the resolution to 45–46 nm and add a noise background similar to the noise measured in the reconstructed images.

3. SUMMARY

We have generated wavelength-resolution soft x-ray holograms using a tabletop setup. The images were numerically reconstructed from a hologram recorded in the surface of a photoresist and digitized with an AFM. This method allows recording of samples without any previous preparation, as required in electron microscopy, and free of the interaction with a probe as occurs in scanning microscopes. Photon-based imaging systems also allow spectroscopic contrast, which is an important characteristic when imaging with shorter wavelength radiation. It also opens the possibility to study specimens in different environments, for example, in the presence of external magnetic or electric fields. Images of carbon nanotubes were obtained with 46 ± 2 nm resolution determined by a knife-edge test. The continued development of highly coherent,

tabletop soft x-ray lasers in the vicinity of 10 nm [18] can be expected to enable future holographic imaging limited only by photoresist resolution. The increasing in flux of soft x-ray tabletop lasers opens the prospect in the future of single-shot recording, permitting full-field time-resolved holographic imaging.

ACKNOWLEDGMENTS

This study was supported by the National Science Foundation (NSF) through the NSF ERC for Extreme Ultraviolet Science and Technology, NSF award no. EEC-0310717.

REFERENCES

1. D. Gabor, "A new microscope principle," *Nature* **161**, 777–778 (1948).
2. A. V. Baez, "A study in diffraction microscopy with special reference to X-Rays," *J. Opt. Soc. Am.* **42**, 756–762 (1952).
3. J. E. Trebes, S. B. Brown, E. M. Campbell, D. L. Matthews, D. G. Nilson, G. F. Stone, and D. A. Whelan, "Demonstration of X-ray holography with an X-ray laser," *Science* **238**, 517–519 (1987).
4. C. Jacobsen, M. Howells, J. Kirz, and S. Rothman, "X-Ray holographic microscopy using photoresists," *J. Opt. Soc. Am. A* **7**, 1847–1861 (1990).
5. S. Lindaas, H. Howells, C. Jacobsen, and A. Kalinovsky, "X-ray holographic microscopy by means of photoresist recording and atomic-force microscope readout," *J. Opt. Soc. Am. A* **13**, 1788–1800 (1996).
6. I. McNulty, J. Kirz, C. Jacobsen, E. H. Anderson, M. R. Howells, and D. P. Kern, "High resolution imaging by Fourier transform X-ray holography," *Science* **256**, 1009–1012 (1992).
7. A. Rosenhahn, R. Barth, X. Cao, M. Schurmann, M. Grunze, and S. Eisebitt, "Vacuum-ultraviolet Gabor holography with synchrotron radiation," *Ultramicroscopy* **107**, 1171–1177 (2007).
8. R. I. Tobey, M. E. Siemens, O. Cohen, M. M. Murnane, H. C. Kapteyn, and K. A. Nelson, "Ultrafast extreme ultraviolet holography: dynamic monitoring of surface deformation," *Opt. Lett.* **32**, 286–288 (2007).
9. P. Wachulak, R. Bartels, M. C. Marconi, C. S. Menoni, J. J. Rocca, Y. Lu, and B. Parkinson, "Sub 400 nm spatial resolution extreme ultraviolet holography with a table top laser," *Opt. Express* **14**, 9636–9642 (2006).
10. P. Wachulak, M. C. Marconi, R. Bartels, C. S. Menoni, and J. J. Rocca, "Volume extreme ultraviolet holographic imaging with numerical optical sectioning," *Opt. Express* **15**, 10622–10628 (2007).
11. CXRO, "<http://www-cxro.lbl.gov/>."
12. B. R. Benware, C. D. Macchietto, C. H. Moreno, and J. J. Rocca, "Demonstration of a high average power tabletop soft X-ray laser," *Phys. Rev. Lett.* **81**, 5804–5807 (1998).
13. C. D. Macchietto, B. R. Benware, and J. J. Rocca, "Generation of millijoule-level soft-x-ray laser pulses at a 4-Hz repetition rate in a highly saturated tabletop capillary discharge amplifier," *Opt. Lett.* **24**, 1115–1117 (1999).
14. U. Schnars and W. P. O. Juptner, "Digital recording and numerical reconstruction of holograms," *Meas. Sci. Technol.* **13**, R85–R101 (2002).
15. P. W. Wachulak, C. A. Brewer, F. Brizuela, W. Chao, E. H. Anderson, R. A. Bartels, C. S. Menoni, J. J. Rocca, and M. C. Marconi, "Simultaneous determination of feature size and resolution in soft x-ray microscopy images," *J. Opt. Soc. Am. B* **25**, B20–B26 (2008).
16. Y. Liu, M. Seminario, F. G. Tomasel, C. Chang, J. J. Rocca, and D. T. Attwood, "Achievement of essentially full spatial coherence in a high-average-power soft-x-ray laser," *Phys. Rev. A* **63**, 033802 (2001).
17. H. H. Solak, D. He, W. Li, S. Singh-Gasson, F. Cerrina, B. H. Sohn, X. M. Yang, and P. Nealey, "Exposure of 38 nm period grating patterns with extreme ultraviolet interferometric lithography," *Appl. Phys. Lett.* **75**, 2328–2330 (1999).
18. Y. Wang, E. Granados, M. A. Larotonda, M. Berrill, B. M. Luther, D. Patel, C. S. Menoni, and J. J. Rocca, "High-brightness injection-seeded soft-x-ray-laser amplifier using a solid target," *Phys. Rev. Lett.* **97**, 123901 (2006).